BJR

■ ARTHRITIS

Promising targets and drugs in rheumatoid arthritis

A MODULE-BASED AND CUMULATIVELY SCORING APPROACH

X. Li,
Y. Yang,
G. Sun,
W. Dai,
X. Jie,
Y. Du,
R. Huang,
J. Zhang

From Tongji Medical College, Huazhong University of Science and Technology, Wuhan, China

Aims

Rheumatoid arthritis (RA) is a systematic autoimmune disorder, characterized by synovial inflammation, bone and cartilage destruction, and disease involvement in multiple organs. Although numerous drugs are employed in RA treatment, some respond little and suffer from severe side effects. This study aimed to screen the candidate therapeutic targets and promising drugs in a novel method.

Methods

We developed a module-based and cumulatively scoring approach that is a deeper-layer application of weighted gene co-expression network (WGCNA) and connectivity map (CMap) based on the high-throughput datasets.

Results

Four noteworthy RA-related modules were identified, revealing the immune- and infection-related biological processes and pathways involved in RA. *HLA-DMA*, *HLA-DMB*, *HLA-DPA1*, *HLA-DPB1*, *HLA-DQB1*, *HLA-DRA*, *HLA-DRB1*, *BLNK*, *BTK*, *CD3D*, *CD4*, *IL2RG*, *INPP5D*, *LCK*, *PTPRC*, *RAC2*, *SYK*, and *VAV1* were recognized as the key hub genes with high connectivity in gene regulation networks and gene pathway networks. Moreover, the long noncoding RNAs (lncRNAs) in the RA-related modules, such as *FAM30A* and *NEAT1*, were identified as the indispensable interactors with the hub genes. Finally, candidate drugs were screened by developing a cumulatively scoring approach based on the selected modules. Niclosamide and the other compounds of T-type calcium channel blocker, IKK inhibitor, and PKC activator, HIF activator, and proteasome inhibitor, which harbour the similar gene signature with niclosamide, were promising drugs with high specificity and broad coverage for the RA-related modules.

Conclusion

This study provides not only the promising targets and drugs for RA but also a novel methodological insight into the target and drug screening.

Cite this article: *Bone Joint Res* 2020;9(8):501–514.

Correspondence should be sent to Dr Jiaming Zhang; email: jiaming_zhang@hsdm.harvard.edu

Article focus

- Some drugs are employed in rheumatoid arthritis (RA) treatment, however some patients respond little and suffer from severe side effects.
- This study is aimed to screen the candidate targets and promising drugs in a novel method.

Key messages

- Four noteworthy RA-related modules were identified, suggesting the immune- and infection-related biological processes and pathways involved in RA.
- *HLA-DMA*, *HLA-DMB*, *HLA-DPA1*, *HLA-DPB1*, *HLA-DQB1*, *HLA-DRA*, *HLA-DRB1*, *BLNK*, *BTK*, *CD3D*, *CD4*, *IL2RG*, *INPP5D*, *LCK*, *PTPRC*, *RAC2*, *SYK*, and *VAV1* were recognized as the key hub genes in RA.
- Long noncoding RNAs *FAM30A* and *NEAT1* were identified as the indispensable interactors with the identified hub genes.

- The candidate drugs were screened by developing a cumulatively scoring approach based on the selected modules.

Strengths and limitations

- This study provides not only the promising targets and drugs for RA but also a novel methodological insight into the target and drug screening.
- The novel method harbours high specificity and broad coverage for the RA-related modules, providing the promising drugs for clinic use.
- Functional research of identified RA-related genes and lncRNAs should be further validated and the pharmacological research of screened compounds should be performed.

Introduction

Rheumatoid arthritis (RA) is a chronic systematic inflammatory and autoimmune disorder with approximately 1% prevalence globally,[1] characterized by synovial inflammation, bone and cartilage destruction, and disease involvement in multiple organs,[2] resulting in joint damage, cardiovascular and pulmonary comorbidity, and malignancy.[3] The joint damage is characterized as persistent and symmetrical polyarthritis and synovial inflammation resulting in cartilage and bone erosion and arthrosis deformity. Although the aetiology of RA is still unclear, a complex interaction of genetic and environmental factors such as diet, ethnicity, smoking, and infection is involved in RA.[4,5]

The treatments of RA are classified into the non-pharmacological treatments and the pharmacological treatments. Non-pharmacological therapy comprises physical and occupational therapy and surgical approaches. Traditional drugs such as glucocorticoids, non-steroidal anti-inflammatory drugs (NSAIDs), and disease-modifying antirheumatic drugs (DMARDs) and new biological drugs including antibodies to pro-inflammatory cytokines (e.g. tumour necrosis factor alpha (TNF-α)) or their receptors (e.g. interelukin (IL)-1, IL-6), or by targeting B-lymphocytes (CD20) or costimulatory molecules (e.g. cytotoxic T-lymphocyte-associated protein 4 (CTLA-4)) are utilized in the treatment of RA.[6] However, some patients respond little to the therapy, and side effects can damage the lives of the patients.

An increasing number of studies have screened the potential targets of RA based on the high-throughput methods, such as microarray profiling[7] and next-generation sequencing.[8] Differentially expressed genes (DEGs) defined by specific thresholds, such as the fold change of gene expression and p-value (e.g. fold change = 2 and p = 0.05), are widely employed in the target screening of RA.[9] However, marginally less significant genes (e.g. foldchange = 1.999 or p = 0.051) are missed, resulting in information loss and bias. Moreover, a different threshold was set among studies, resulting in

inconsistence of screened targets. Co-expression networks or protein-protein interaction networks constructed by external public databases, such as STRING and BioGRID, are also applied to target screening.[10] Due to the ignorance of indirect gene interactions or indeterminacy of public databases based on different algorithms and data sources, the limitation of this method is obvious. To avoid these limitations, Langfelder et al[11] developed the weighted gene co-expression network analysis (WGCNA) method, which applies the soft-threshold and considers the indirect interactions between genes, and constructs weighted gene regulation network to find biologically relevant modules and genes. Based on this method, Ma et al[12] identified the critical genes in RA such *CD97*, *FYB*, and *CXCL1*.

The connectivity map (CMap) is a useful tool to build the link between disease and compounds by comparing microarray data from more than 1,300 small molecules to the gene signature of the phenotype using a pattern-matching algorithm with a high level of resolution and specificity, which allows for the screening of candidate drugs.[13,14] CLUE, the next generation CMap, is a platform for the analysis of perturbational datasets generated using gene expression (L1000) and proteomic (P100 and GCP) assays, which integrate the CMap dataset and provide the useful tool Touchstone (Broad Institute, Cambridge, Massachusetts, USA) to assess and visualize connectivity among perturbagens.[15] Touchstone was utilized to investigate the compounds with the similar signature by ranking the median enrichment score (MES) and clustering based on the gene expression signature among multiple types of cell.

Based on the microarray datasets, this study constructed a weighted gene network to identify the significant RA-related modules and genes to investigate the pathogenesis and therapeutic targets. Moreover, we screened promising compounds for the clinical treatment of RA by developing a module-based and cumulatively scoring approach that ensured high specificity and broad coverage for RA-related modules. Our study provides an insight into the novel bioinformatic approach utilized in the target and drug screening for RA.

Methods

Data collection and pre-processing. The datasets GSE55235, GSE55457, and GSE55584 were included by the criteria of "rheumatoid arthritis", "human", and "synovial or synovium" and obtained from the National Centre For Biotechnology Information (NCBI) Gene Expression Omnibus (GEO).[7] The microarray datasets included in this study are based on the platform of Affymetrix Human Genome U133A Array (HG-U133A), which is designed to analyze the expression level of 18,400 transcripts and variants by a probe hybridization method and composed of more than 22,000 probes. The datasets contain 53 synovial tissues from 33 RA patients and 20 healthy donors, respectively. The clinical information is shown
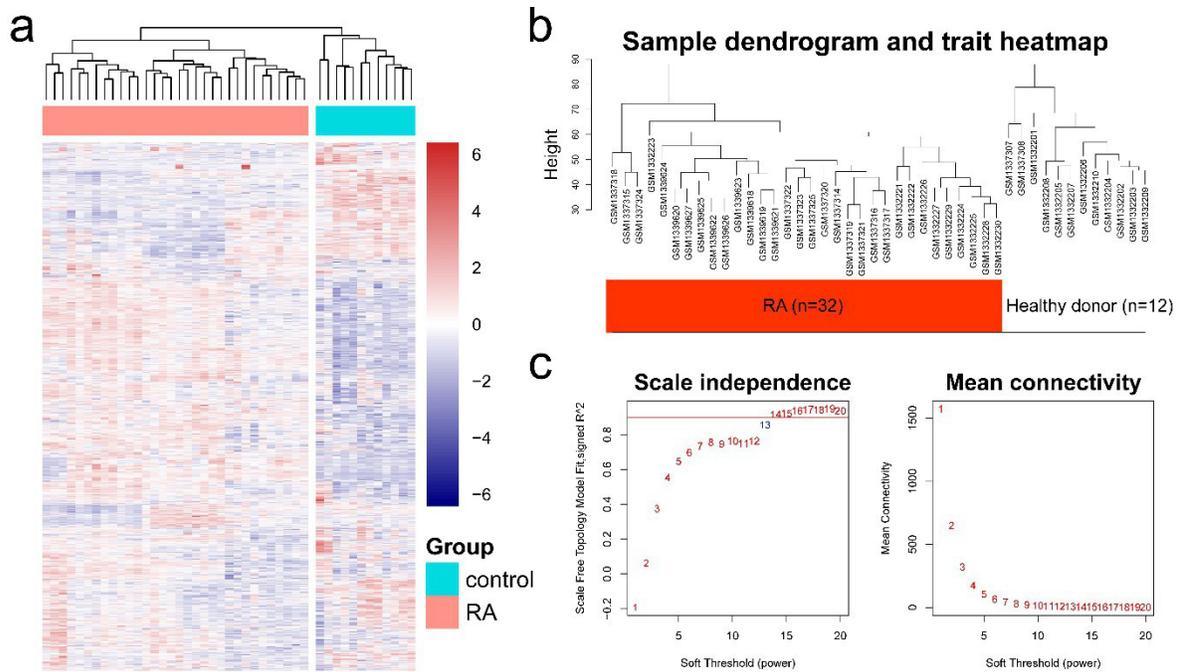
Fig. 1

Sample clustering and soft-thresholding power determination. a) Heatmap plot of the top 25% genes in rank of variance. b) Sample clustering dendrogram of the joint synovial samples of 32 rheumatoid arthritis (RA) patients and 12 healthy donors. The samples clustered based on their Euclidean distance calculated with variance stabilized expression levels. c) Analysis of the scale-free fit index for various soft-thresholding powers.

in Supplementary Table S1. Background correction and quantile normalization were performed by Robust multi-array analysis method.[16] Batch effect was carefully considered by R package BatchI (v2.0; R Foundation for Statistical Computing, Vienna, Austria).[17] Medians were considered as gene expression values if the multiple probes were mapped to the same gene symbol.

Weighted gene co-expression network analysis. Considering the capacity and stability of bioinformatics statistics, the top 25% genes in the rank of the variance of expression were selected to build the gene network by R package WGCNA (v1.69; R Foundation for Statistical Computing).[11] Firstly, an essential parameter to build the scale-free network, soft-thresholding power, was determined by functions softConnectivity and pickSoftThreshold. In brief, the influence of power values on the mean connectivity and scale independence was analyzed by these functions. The function softConnectivity calculated the network connectivity, and the function pickSoftThreshold calculated the scale-free topology fit index for different powers. When the scale-free topology fit index reaches 0.9 at the powers < 30 and the network harboured an appropriate network connectivity, the soft-thresholding power was determined, at which the topology network was considered scale-free and suitable for further analysis. Then, the adjacency matrix was converted into Topological Overlap Matrix (TOM), in which parts of genes harbouring the high topological overlap with others were hierarchically

clustered. With the parameters set up as minModuleSize = 30 and deepsplit = 2, the modules were identified by Dynamic Tree Cut algorithm. Based on the module eigengene calculated to represent the modules in a 1D vector, the close modules are merged by hierarchical clustering and Merged Dynamic algorithm (cutheight = 0.25). Finally, the eigengenes were used to calculate the correlation between the modules and RA. In addition, the Pearson correlation coefficient was calculated to quantify the correspondence between modules and RA, and to identify the RA-related modules with the criterions of the Pearson correlation coefficient $r > 0.4$ and $p < 0.05$.

Functional enrichment analysis. R package ClusterProfiler (v3.14.3; R Foundation for Statistical Computing) was used to analysis the Gene Ontology (GO) and Kyoto Encyclopedia of Genes and Genomes (KEGG) to annotate RA-related modules.[18] Based on hypergeometric distribution, the functions enrichGO and enrichKEGG were utilized to perform enrichment test for GO terms and KEGG pathways, the results of which were visualized by bubble plot. The heatmap of enriched genes and the regulation network of enriched genes and relevant pathways were plotted by function heatplot and KEGGcnetplot, respectively.

Hub gene and long noncoding RNA identification. Hub genes are the key regulators with high degree or connectivity in the scale-free network. In order to identify the hub genes in the RA-related modules, three

a

b

Cluster Dendrogram

c

d
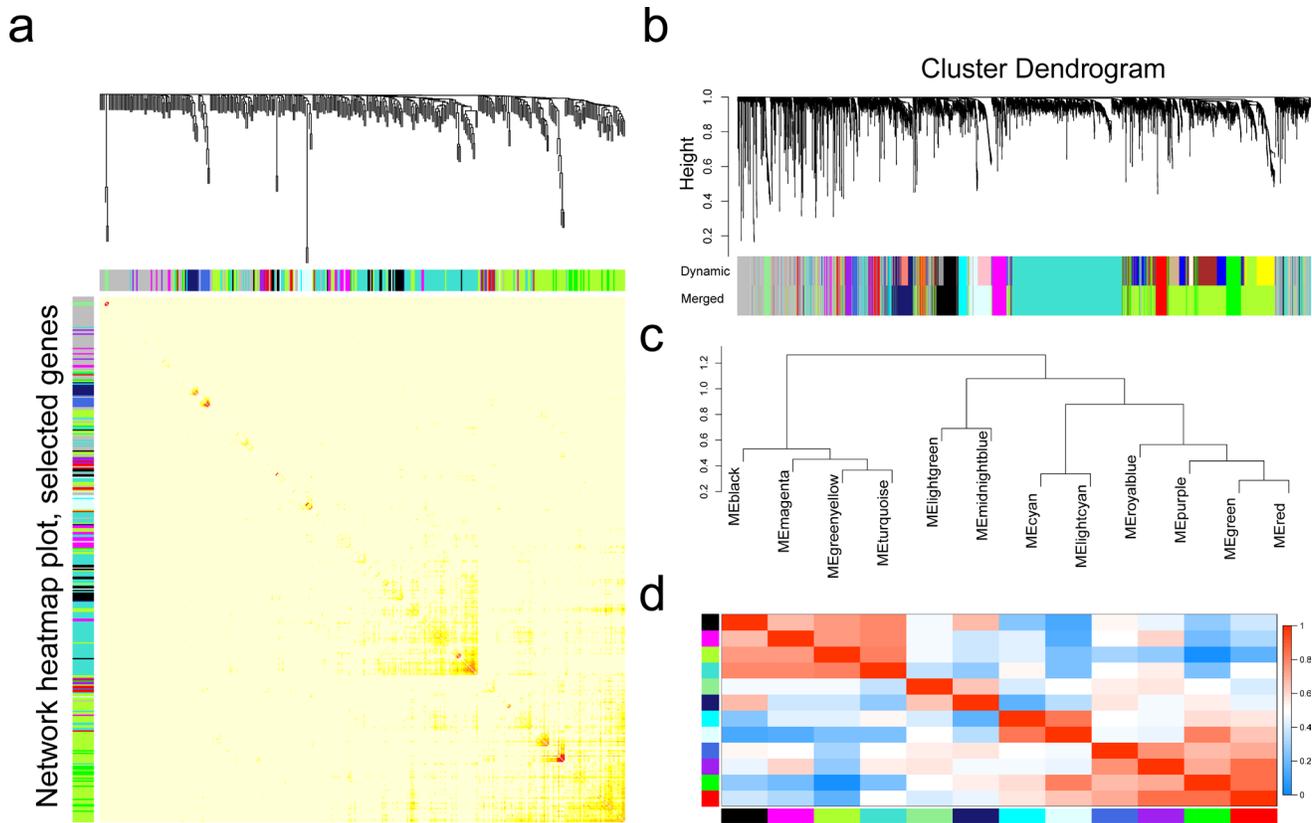
Fig. 2

Topological overlap calculation and module identification. a) Heatmap plot of topological overlap in the gene network. Red squares along the diagonal correspond to modules. b) Gene dendrogram calculated by average linkage hierarchical clustering. The colour row underneath the dendrogram shows the assigned original module and the merged module. c) Hierarchical clustering of module eigengenes that summarize the modules identified in the clustering analysis. d) Heatmap plot of the eigengene adjacencies. Each row and column in the heatmap corresponds to one module eigengene.

parameters including Gene Significance (GS), Module Membership (MM), and the degree in the RA-related module were utilized. GS reflects the inter-relation between genes and sample traits. MM reflects the inter-relation between the genes and module eigengenes. Degree determines the gene connectivity in the network. Hub genes were defined as the intersection of the top 10% genes in the rank of the degree and the genes with both the absolute values of MM and GS both larger than 0.7 and the p-value less than 0.01, harbouring high connectivity both in the gene-phenotype mapping and gene co-expression networks. The probe IDs of the platform of Affymetrix Human Genome U133A Array (HG-U133A) were converted to ENSG IDs annotated by Ensembl database (Release 98; European Molecular Biology Laboratory's European Bioinformatics Institute (EMBI-EBI), Hinxton, UK) and then 106 lncRNAs were identified based on Ensembl database (Release 98) and verified by NONCODE database (v5.0),[19] the regulatory networks of which were constructed and visualized by Cytoscape (Institute for Systems Biology (ISB), Seattle, Washington, USA).

Compound screening based on modules. CMap is a powerful tool for screening of compounds against a genome-wide disease or physiological gene signature by comparing microarray data from more than 1,300 small molecules to the gene signature of the phenotype of interest using a pattern-matching algorithm with a high level of resolution and specificity.[13,14] To find the potential therapeutic compound with high specificity and broad coverage for the RA-related modules, we mapped the gene expression signature of each module to CMap to link the compounds to the modules and performed the intersection of the compounds targeting the corresponding module. Enrichment scores, used to quantize the similarity between the gene expression signature of compounds and modules, were adjusted by the module-trait correlation coefficient, generating an integrated score, namely the module-adjusted score (MAS), to evaluate the connectivity of compounds and RA. The MAS is calculated using the following formula:

$$MAS = \sum Enrichment\ score \times module\text{-}trait\ correlation\ coefficient.$$

a

b

Fig. 3
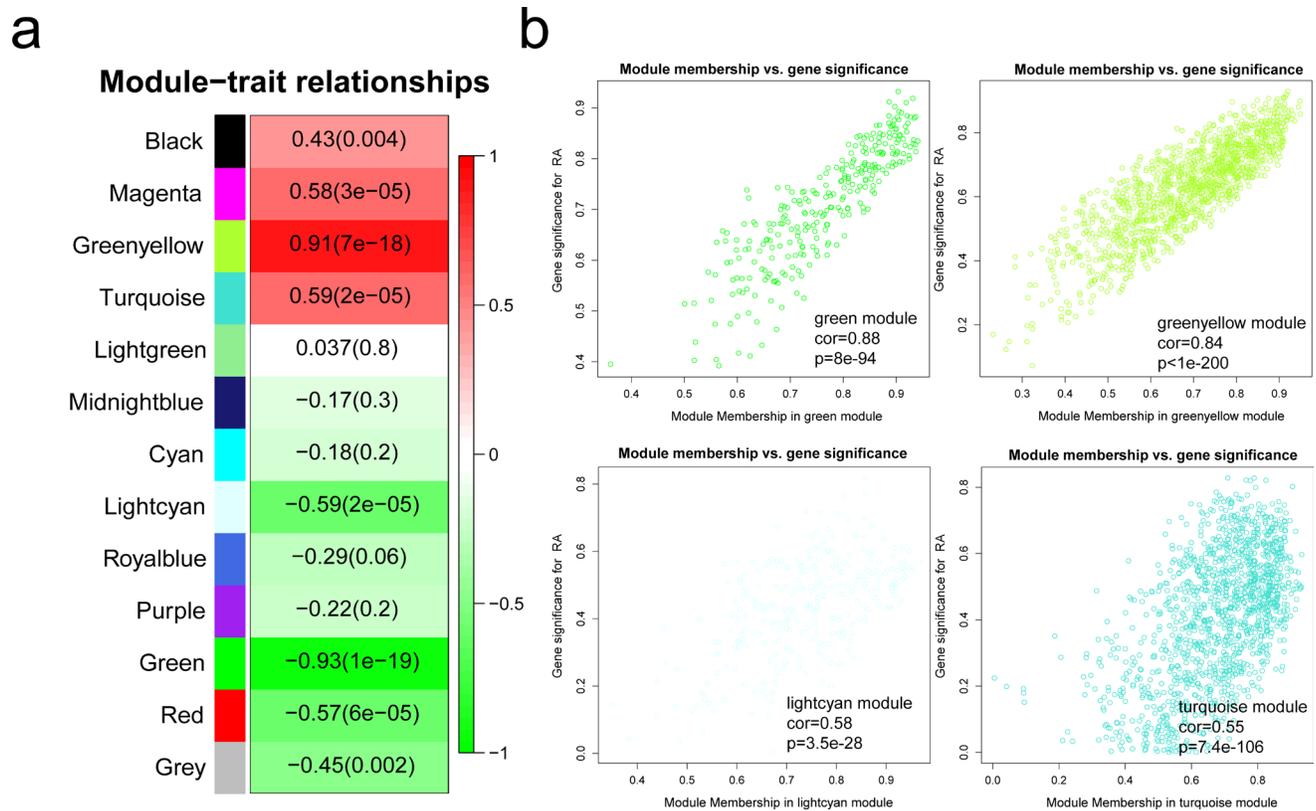
Identification of modules associated with rheumatoid arthritis (RA). a) Heatmap of the correlation between module eigengenes and RA. The value in each square and the p-value in parentheses reflect the correlation coefficient between the module eigengene and RA.
b) Scatter plot for correlation between gene significance (GS) and gene module membership (MM) in RA-related modules (green, greenyellow, lightcyan, and turquoise). All p-values were calculated using one-way analysis of variance and Pearson correlation coefficient.

Results

Data processing and soft-thresholding power determination. The gene expression matrices were obtained after profile pre-processing (background correction and normalization). To identify the potential outliers, samples were clustered based on the corresponding expression matrices. The dendrogram of the hierarchical clustering is shown in Supplementary Figure S1. A total of eight normal samples and one RA sample were identified as the outliers and removed from the analysis. As shown in Figures 1a and 1b, the sample clustering revealed the high correlation of the phenotypes and expression profiles after excluding the outliers. Among the 22,283 probes in expression profile (Affymetrix Human Genome U133A Array), the top 25% genes in the rank of the expression variance were selected to perform the analysis of the network topology for different powers in order to balance the mean connectivity and scale independence. As shown in Figure 1c, the power of 13 is the lowest power for which the scale-free topology fit index reaches 0.90.

Weighted co-expression network and RA-related module identification. With the soft-thresholding power of 13, the scale-free topology model was constructed and the adjacency matrix was converted into a TOM

(Figure 2a). A total of 21 modules were identified by average linkage hierarchical clustering of gene expression and dynamic tree cut method, which were subsequently merged to 13 modules by module eigengene clustering (Figure 2b). The module eigengene calculated by the first principal component to represent each module was applied to analyze the correlation of each module (Figure 2c and 2d). To identify the RA-related modules, the correlation between module eigengene and RA was calculated by one-way analysis of variance (ANOVA) (significant p-value < 0.05). As shown in Figure 3a, the green module showed the highest correlation with RA ($r = -0.93$; $p = 1e-19$, one-way ANOVA). Besides, the greenyellow module ($r = 0.91$; $p = 7e-18$, one-way ANOVA), the lightcyan module ($r = -0.59$; $p = 2e-05$, one-way ANOVA), and the turquoise module ($r = 0.59$; $p = 2e-05$, one-way ANOVA) were also relevant to RA. Due to the high relevance for RA ($|r| > 0.9$), the green module and the greenyellow module were selected as modules of interest and studied in subsequent analyses.

Functional annotation of RA-related modules. In order to explore the biological relevance of RA-related modules, 282 genes in the green module and 1,263 genes
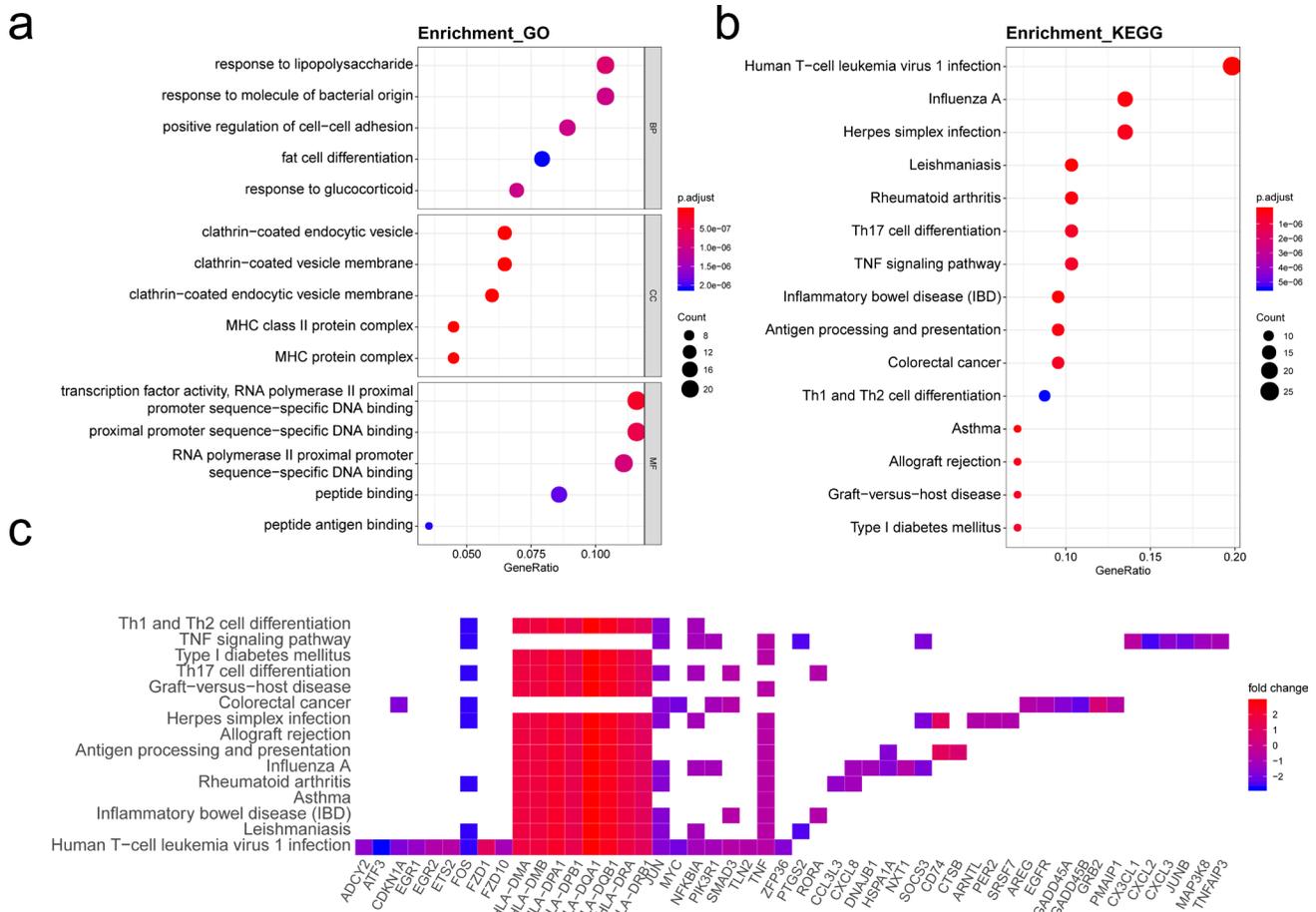
Fig. 4

Functional annotation of green module. a) Gene ontology (GO) term enrichment and b) Kyoto Encyclopedia of Genes and Genomes (KEGG) pathway analysis of green module. GeneRatio indicates the gene number ration in each of the GO functions and KEGG pathways. The colour and size of each dot represents a p-value (calculated by independent-samples *t*-test and adjusted using the Benjamini and Hochberg method and gene number assigned to the corresponding GO term and KEGG pathway, respectively. c) Heatmap plot of enriched genes in KEGG pathways. BP, biological process; CC, cellular component; MF, molecular function; MHC, major histocompatibility complex; Th, T helper cell; TNF, tumour necrosis factor.

in the greenyellow module were subjected to GO functional and KEGG pathway enrichment analyses. With the threshold of p-value adjusted by Benjamini and Hochberg method less than 0.05, the biological processes of the green module were mainly involved in the response to lipopolysaccharide (p = 2.21e-10, independent-samples *t*-test), the response to molecule of bacterial origin (p = 5.88e-10), the positive regulation of cell-cell adhesion (p = 1.15e-09), the response to glucocorticoid (p = 1.16e-09), and fat cell differentiation (p = 2.99e-09) (Figure 4a). In the KEGG analysis, the green module was mainly involved in the infection-related pathways including human T-cell leukaemia virus 1 infection (p = 6.08e-13) and leishmaniasis (p = 2.32e-10) and the immune-related pathways such as inflammatory bowel disease (p = 6.48e-10), asthma (p = 1.31e-09), and RA (p = 2.89e-09) (Figure 4b). Major histocompatibility complex Class II (MHC Class II) genes including *HLA-DMA*, *HLA-DMB*,

HLA-DPA1, *HLA-DPB1*, *HLA-DQB1*, *HLA-DRA*, and *HLA-DRB1* exhibited high connectivity to the enriched pathways in the green module (Figure 4c).

The greenyellow module was mainly involved in the immune-related biological processes including the immune response-regulating cell surface receptor signalling pathway (p = 2.86e-32, independent-samples *t*-test and adjusted by Benjamini and Hochberg method), the regulation of lymphocyte activation (p = 4.25e-32), immune response-activating cell surface receptor signalling pathway (p = 3.19e-31), the positive regulation of cell activation (p = 6.20e-29), and B cell activation (p = 6.95e-29) (Figure 5a). In the KEGG pathway analysis, the greenyellow module showed strong relevance to Fc γ R (FcγR)-mediated phagocytosis (p = 3.40e-11), osteoclast differentiation (p = 7.65e-11), phagosome (p = 4.96e-10), haematopoietic cell lineage (p = 9.37e-10), and primary immunodeficiency (p = 7.02e-09) (Figure 5b). Fc fragment of immunoglobulin G (IgG) receptors in the most
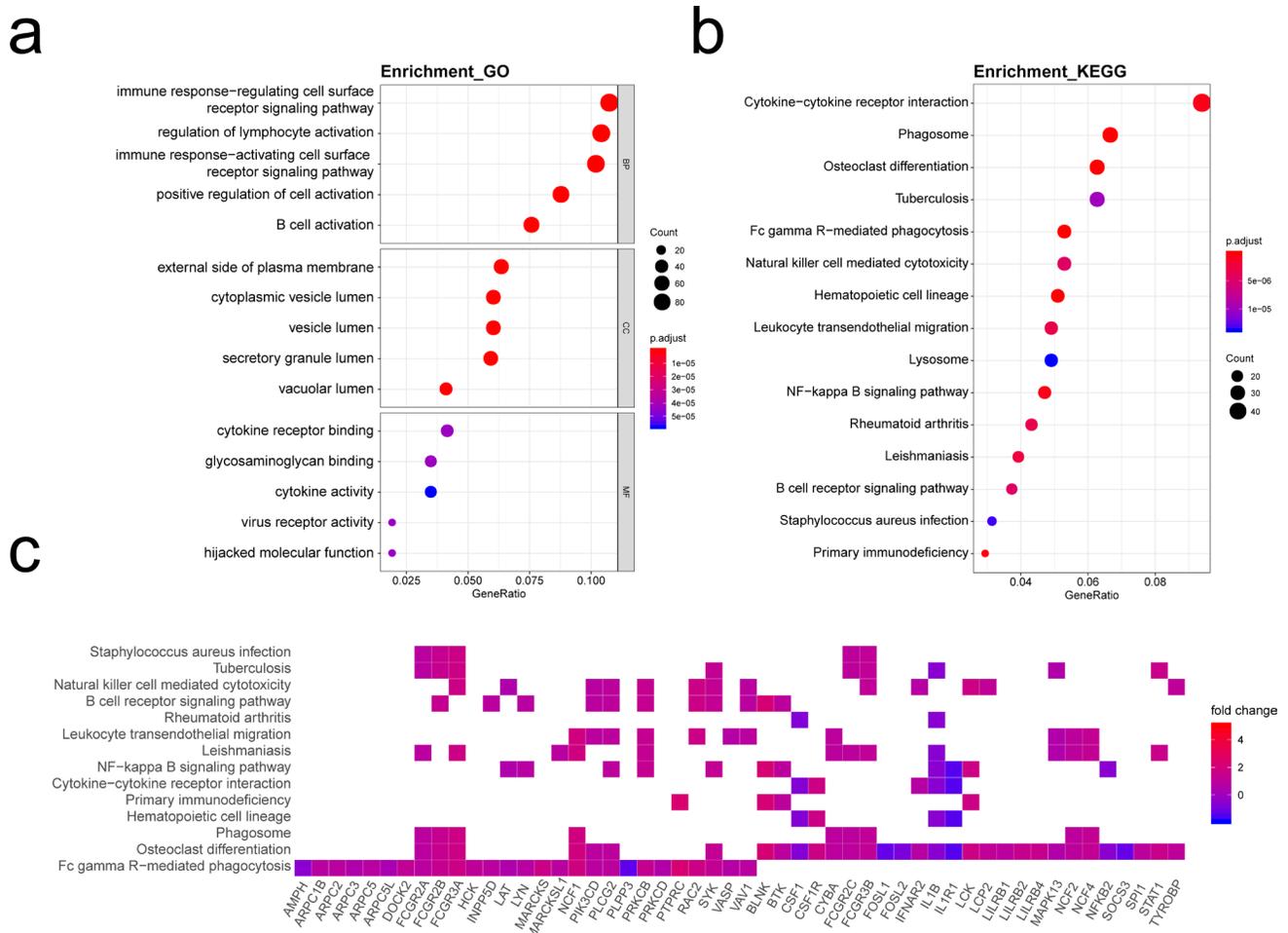
Fig. 5

Functional annotation of greenyellow module. a) Gene ontology (GO) term enrichment and b) Kyoto Encyclopedia of Genes and Genomes (KEGG) pathway analysis of greenyellow module. GeneRatio indicates the gene number ration in each of the GO functions and KEGG pathways. The colour and size of each dot represents a p-value adjusted using the Benjamini and Hochberg method and gene number assigned to the corresponding GO term and KEGG pathway, respectively. c) Heatmap plot of enriched genes in KEGG pathways. BP, biological process; CC, cellular component; MF, molecular function; NF-kappa B, nuclear factor kappa-light-chain-enhancer of activated B cells.

significant enriched pathway, including *FCGR2A*, *FCGR2B*, and *FCGR3A*, also participated in other module-related pathways such as osteoclast differentiation and phagosome (Figure 5c).

Identification of hub genes in RA-related modules. The hub genes were defined as the genes with high connectivity both in gene regulation network and gene-phenotype mapping. The intersection of the top 10% genes in the rank of degree and the genes with both the absolute value of MM and GS larger than 0.7 and p-value less than 0.01 was identified as the hubs in the RA-related modules. In the green module, all the genes with top 10% degree had high |MM| and |GS| (Figure 6a), among which MHC Class II genes including *HLA-DMA* (log$_2$FC = 1.79; p = 1.10e-12, calculated by independent-samples *t*-test and adjusted by Benjamini and Hochberg method), *HLA-DMB* (log$_2$FC = 1.86; p = 8.25e-17), *HLA-DPA1* (log$_2$FC = 1.21; p = 2.31e-08), *HLA-DPB1* (log$_2$FC = 1.51; p = 8.35e-12),

HLA-DQB1 (log$_2$FC = 2.28; p = 1.82e-09), *HLA-DRA* (log$_2$FC = 1.67; p = 9.95e-12), and *HLA-DRB1* (log$_2$FC = 1.19; p = 4.09e-11) were identified as the core hubs because of their high connectivity to the significant pathways in the green module (Figure 6b and Table I). In the greenyellow module, 120 genes were recognized as the hub genes (Figure 6c), among which *BLNK* (log$_2$FC = 2.20; p = 8.86e-15), *BTK* (log$_2$FC = 0.79; p = 1.58e-11), *CD3D* (log$_2$FC = 1.72; p = 8.59e-09), *CD4* (log$_2$FC = 1.02; p = 2.99e-11), *IL2RG* (log$_2$FC = 1.15; p = 2.26e-08), *INPP5D* (log$_2$FC = 0.88; p = 1.09e-09), *LCK* (log$_2$FC = 1.69; p = 8.76e-09), *PTPRC* (log$_2$FC = 2.11; p = 2.38e-10), *RAC2* (log$_2$FC = 1.07; p = 1.11e-05), *SYK* (log$_2$FC = 1.25; p = 2.55e-11), and *VAV1* (log$_2$FC = 0.90; p = 8.32e-09) were identified as the core hubs functionally relevant to the greenyellow module (Figure 6d and Table I).

Identification of lncRNAs in RA-related modules. Long noncoding RNAs (lncRNAs) are emerging players in
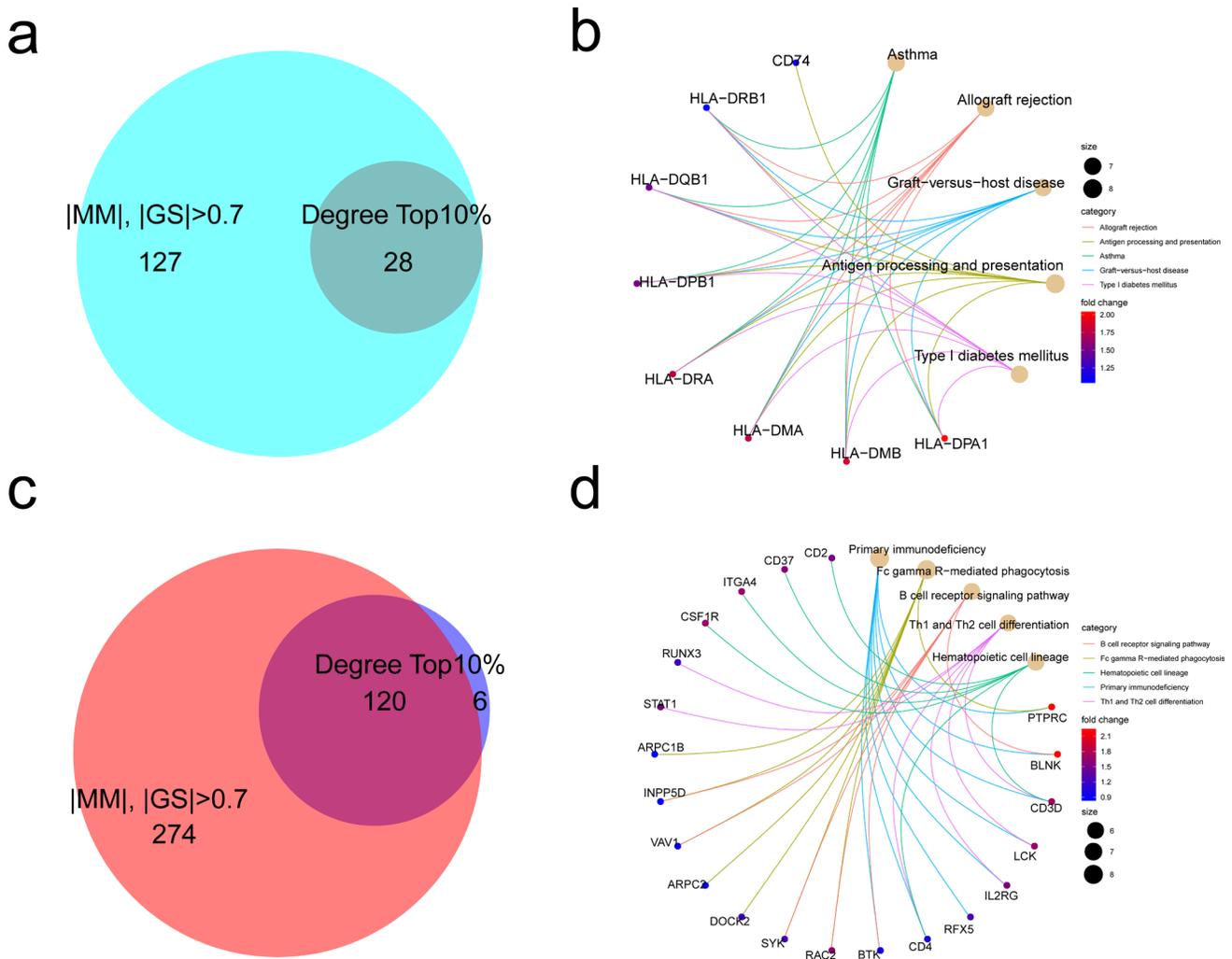
Fig. 6

Identification of hub genes in rheumatoid arthritis (RA)-related modules. The overlap of top 10% genes in the rank of degree and the genes with both absorb value of Module Membership (MM) and Gene Significance (GS) larger than 0.7 and p-value larger than 0.01 in the a) green module and c) greenyellow module. The hub genes related to enriched pathways are shown in the b) green module and d) greenyellow module. Th, T helper cell.

various diseases, such as RA and osteoarthritis. A total of six lncRNAs were identified in the greenyellow and lightcyan modules, including *FAM30A* ($\log_2$FC = 0.75; p = 3.63e-03, calculated by independent-samples *t*-test and adjusted by Benjamini and Hochberg method), *NEAT1* ($\log_2$FC = −1.63; p = 7.64e-06), *MEG3* ($\log_2$FC = −0.86; p = 3.55e-05), *SND1-IT1* ($\log_2$FC = −0.41; p = 3.32e-03), *SNHG17* ($\log_2$FC = −0.83; p = 7.41e-06), and *THAP9-AS1* ($\log_2$FC = −0.58; p = 3.28e-04), among which *FAM30A* in the greenyellow module and *NEAT1* in the lightcyan module were recognized as the significant regulators with the high degree of 127 and 73, respectively (Table II).

To further investigate their roles in RA, the regulation networks of lncRNAs were constructed, in which the lncRNA-related genes were subjected to the functional annotation. As shown in Figure 7a, a total of 66 genes were identified as the *FAM30A*-related genes in the greenyellow module, which were functionally involved in the module-related pathways mentioned above, such

as primary immunodeficiency, T helper type 1 (Th1) and Th2 cell differentiation, and human T-cell leukaemia virus 1 infection, suggesting an indispensable role of *FAM30A* in the greenyellow module (Figure 7c). Moreover, the hub genes *CD3D*, *IL2RG*, and *LCK* were identified in the *FAM30A*-regulation network. In the lightcyan module, 44 *NEAT1*-related genes were identified and found to be involved in the adherent junction, parathyroid hormone, and mitogen-activated protein kinase (MAPK) pathways, among which *FGFR1* showed the highest degree of the enriched pathways (Figures 7b and 7d). However, no lncRNAs were identified in the green module or turquoise module.

Compound screening based on RA-related modules. Using a pattern-matching algorithm, the CMap links compounds with disease or physiological phenotypes by measuring similarities in gene expression. To screen the potential therapeutic compounds with high specificity for RA, we mapped the gene expression signature of each module to CMap and constructed the relations

Table I. Hub genes in rheumatoid arthritis-related modules.

Gene symbol	ENSG ID	log2FC	P.log2FC*	GS	P.GS†	MM	P.MM†	Pathway‡	Module
BLNK	ENSG00000095585	2.20	8.86E-15	0.86	5.59E-14	0.89	3.05E-16	2	greenyellow
BTK	ENSG00000010671	0.97	1.58E-11	0.81	4.34E-11	0.91	2.28E-17	2	greenyellow
CD3D	ENSG00000167286	1.72	8.59E-09	0.73	2.45E-08	0.88	2.81E-15	3	greenyellow
CD4	ENSG00000010610	1.02	2.99E-11	0.80	8.58E-11	0.90	6.83E-17	3	greenyellow
IL2RG	ENSG00000147168	1.54	2.26E-08	0.71	6.01E-08	0.85	3.32E-13	2	greenyellow
INPP5D	ENSG00000168918	0.88	1.09E-09	0.76	2.55E-09	0.89	4.52E-16	2	greenyellow
LCK	ENSG00000182866	1.69	8.76E-09	0.73	2.49E-08	0.86	1.08E-13	2	greenyellow
PTPRC	ENSG00000081237	2.11	2.38E-10	0.77	8.55E-10	0.91	1.40E-17	2	greenyellow
RAC2	ENSG00000128340	1.07	1.11E-05	0.60	2.02E-05	0.76	3.04E-09	2	greenyellow
SYK	ENSG00000165025	1.25	2.55E-11	0.80	8.55E-11	0.90	7.71E-17	2	greenyellow
VAV1	ENSG00000141968	0.90	8.32E-09	0.73	1.89E-08	0.89	1.11E-15	2	greenyellow
HLA-DMA	ENSG00000204257	1.79	1.10E-12	0.83	5.03E-12	-0.92	3.35E-18	5	green
HLA-DMB	ENSG00000242574	1.86	8.25E-17	0.89	5.91E-16	-0.91	1.54E-17	5	green
HLA-DPA1	ENSG00000231389	1.21	2.31E-08	0.71	5.78E-08	-0.83	3.02E-12	5	green
HLA-DPB1	ENSG00000223865	1.51	8.35E-12	0.81	3.25E-11	-0.90	1.53E-16	5	green
HLA-DQB1	ENSG00000179344	2.28	1.82E-09	0.75	5.89E-09	-0.85	1.52E-13	5	green
HLA-DRA	ENSG00000204287	1.67	9.95E-12	0.81	3.99E-11	-0.92	5.56E-19	5	green
HLA-DRB1	ENSG00000196126	1.19	4.09E-11	0.79	1.31E-10	-0.91	3.00E-17	5	green

FC, the fold change of rheumatoid arthritis (RA) compared to healthy donors; GS, gene significance; MM, gene module membership. P.log$_2$FC, P.GS, and P.MM represent the p-values of log$_2$FC, MM, and GS, respectively.
*Calculated by independent-samples t-test and adjusted by Benjamini and Hochberg method.
†Pearson correlation coefficient.
‡The enriched pathway numbers of hub genes.

Table II. Long noncoding RNAs in rheumatoid arthritis-related modules.

Gene symbol	ENSG ID	log2FC	P.log2FC*	MM	P.MM*	GS	P.GS*	Degree†	Module
FAM30A	ENSG00000226777	0.75	3.63E-03	0.55	1.21E-04	0.42	4.81E-03	127	greenyellow
NEAT1	ENSG00000245532	-1.63	7.64E-06	0.58	4.01E-05	-0.60	1.48E-05	73	lightcyan
MEG3	ENSG00000214548	-0.86	3.55E-05	0.53	2.36E-04	-0.57	5.92E-05	49	lightcyan
SND1-IT1	ENSG00000279078	-0.41	3.32E-03	0.28	6.39E-02	-0.42	4.11E-03	49	lightcyan
SNHG17	ENSG00000196756	-0.83	7.41E-06	-0.54	1.45E-04	-0.61	1.31E-05	5	greenyellow
THAP9-AS1	ENSG00000251022	-0.58	3.28E-04	-0.45	2.01E-03	-0.51	4.63E-04	2	greenyellow

FC, the fold change of RA compared to healthy donors; GS, gene significance; MM, gene module membership. P.log$_2$FC, P.GS, and P.MM represent the p-values of log$_2$FC, MM, and GS, respectively.
*Calculated by independent-samples t-test and adjusted by Benjamini and Hochberg method.
†The degree or connectivity of hub long noncoding RNAs in corresponding module.

of modules and compounds. As shown in Figure 8, 35, 47, 36, and 24 compounds were identified to target the green, greenyellow, lightcyan, and turquoise modules, respectively. To find the compounds targeting to as many modules as possible, we took the intersection of the compounds targeting the RA-related modules (Figure 8a). Moreover, we adjusted the enrichment scores of compounds by module-trait correlation coefficient and constructed the weighted compound-phenotype relations. The top 20 compounds in the rank of the MAS were identified as the potential therapeutic drugs with high specificity and broad coverage for the RA-related modules (Table III), among which niclosamide had the highest score of 2.01057. To assess the clinical value and mechanisms of niclosamide, we further investigated the compounds with similar signature to niclosamide, among which the top ten compounds in the rank of MES were clustered based on the expression signature in multiple types of cell, including A375 (human malignant melanoma), HA1E (human renal epithelial cell), HCC515 (human lung carcinoma), A549 (human non-small cell carcinoma), PC3 (human prostate adenocarcinoma), MCF7 (breast adenocarcinoma), and VCAP (prostate adenocarcinoma) (Figure 8b). Heliomycin harboured the most similar signature pattern with niclosamide among the multiple types of cells and IKK2-inhibitor-V harboured the highest MES. Compound categories were also investigated by clustering the compounds with the similar gene expression signature to niclosamide. As shown in Figure 7c, T-type calcium channel blocker (MES = 99.78, compound number = 5), IKK inhibitor (MES = 99.68, compound number = 3), PKC activator (MES = 99.74, compound number = 5), HIF activator (MES = 99.64, compound number = 4), and proteasome inhibitor (MES = 99.45, compound number = 3) were the top five categories in the rank of MES.
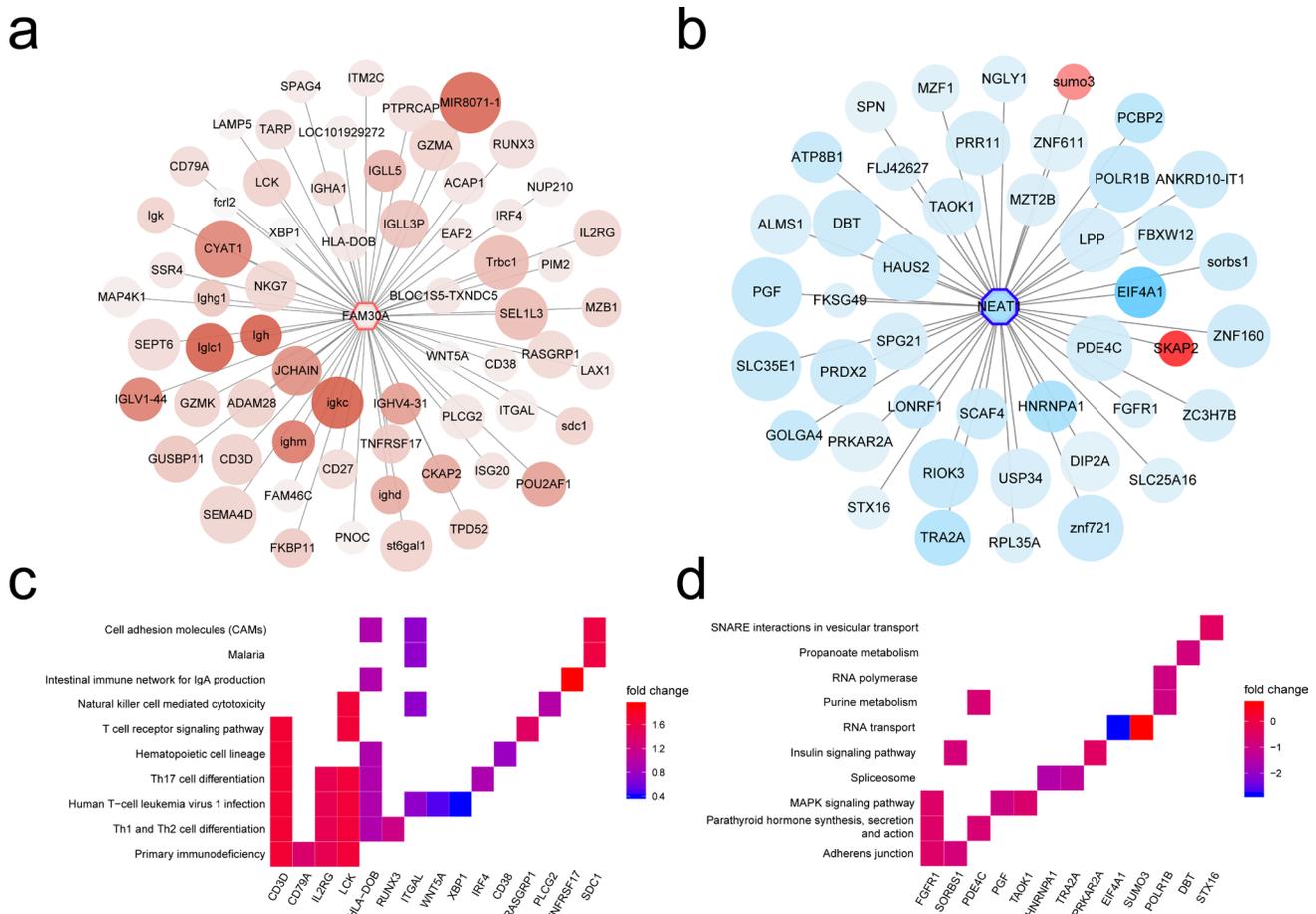
Fig. 7

Identification of hub long noncoding RNAs (lncRNAs) in rheumatoid arthritis (RA)-related modules. a) The co-expression regulation network of lncRNA FAM30A in greenyellow module. b) The co-expression regulation network of lncRNA NEAT1 in lightcyan module. c) Heatmap plot of enrich genes of Kyoto Encyclopedia of Genes and Genomes (KEGG) pathways in FAM30A-regulated network. (d) Heatmap plot of enrich genes of KEGG pathways in NEAT1-regulated network. IgA, immunoglobulin A; MAPK, mitogen-activated protein kinase; SNARE, SNAP REceptor; Th, T helper cell.

Discussion

Rheumatoid arthritis is a systematic autoimmune disorder, the aetiology of which is still unclear. In this study, we performed WGCNA analysis based on the microarray datasets from a multicentre study including 33 RA patients and 20 healthy donors. Four significant RA-related modules were identified in our results, the functional annotation of which revealed the important pathways in RA.

The role of pathogens in the pathogenesis of RA is increasingly being recognized. Virus is identified as an important factor triggering autoimmunity in genetically susceptible patients and leading to diseases such as RA, Sjögren's syndrome, antiphospholipid syndrome, and systemic lupus erythematosus (SLE).[20] The infection of human T-cell leukaemia virus type-1 or human T-lymphotropic virus type-1 (HTLV-1) was involved in the development of RA.[21] HTLV-1-positive RA patients were subjected to higher inflammation and greater resistance to anti-TNF treatment.[22] Büchel et al[23] revealed a relationship between the influenza-A pathway and RA

by an integrative pathway-based approach for genome-wide association studies (GWAS). Although no significant difference was determined for the serologic markers of herpes simplex viruses (HSV) in RA compared to the control group,[24] HSV infection acts as a trigger of autoimmunity resulting in autoimmune diseases such as post-herpes simplex encephalitis, Guillain-Barré syndrome, and Bell's palsy.[24-26] Moreover, the enriched items such as Th17 cell differentiation, response to lipopolysaccharide and molecule of bacterial origin, and leishmaniasis revealed the indispensable role of bacteria in RA. Bacteria are also important pathogens in triggering autoimmunity. Th17 lineage cells, which function in the clearance of extracellular bacterial infections, play important roles in autoimmune disorders including inflammatory bowel disease and RA.[27] Serum markers of RA, including rheumatoid factor and anti-cyclic citrullinated peptide antibody, were detected in visceral leishmaniasis,[28] which may suggest the relevance between leishmaniasis and RA.
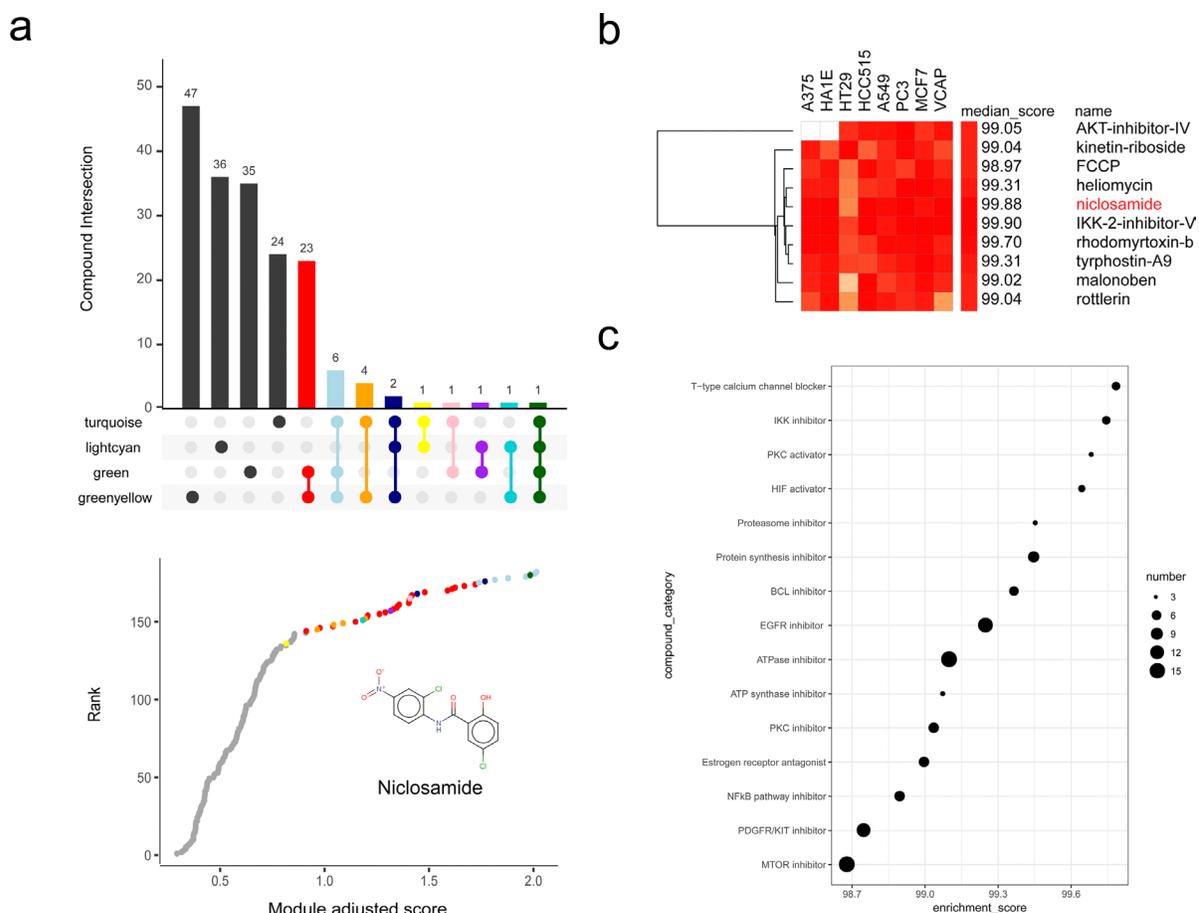
Fig. 8

Compound screening based on rheumatoid arthritis (RA)-related modules. a) Intersection of compounds targeting to specific RA-related modules and enrichment scores adjusted by module-trait correlation coefficient. b) Heatmap of gene expression signature of niclosamide and the compounds with similar signature. c) Compound categories with similar gene expression signature to niclosamide. EGFR, epidermal growth factor receptor; mTOR, mammalian target of rapamycin; NFκB, nuclear factor kappa-light-chain-enhancer of activated B cells; PDGFR, platelet-derived growth factor receptor; PKC, protein kinase C.

The role of immune disorders in RA has been widely recognized. Phagocytosis is an essential element of the immune response in the elimination of pathogens, cellular debris, apoptotic cells, and tumour cells.[29] FcγR-mediated phagocytosis and lysosome were proven to be involved in four common autoimmune diseases, including Type 1 diabetes mellitus (T1D), multiple sclerosis (MS), SLE, and RA.[30,31] The expression of FcγRI and FcγRII on monocytes was elevated in the RA patients compared with healthy controls,[32] and FcγRIIA polymorphism contributes to the course of RA.[33] The imbalance between activating and inhibitory FcγRs on macrophages, a deciding factor for the cellular response to immune complexes (ICs), is crucial in modulating the synovial inflammation.[34] T and B lymphocytes also play a pathological role in the development and propagation of RA.[35] B lymphocytes are recruited to the synovial fluid, where they contribute to local inflammation through the secretion of pro-inflammatory cytokines, the production of autoreactive pathogenic antibodies, and the antigen presentation for autoreactive T cells.

In this study, we recognized hub genes by two criterions, including the degrees in co-expression networks and the GS for RA. Almost all of the top 10% genes in the rank of degree show high GS. Given that we assumed the core hub gene should be functionally relevant in the module, we constructed the hub gene pathway networks and screened for the more critical cores among hundreds of hub genes. MHC Class II genes including *HLA-DMA*, *HLA-DMB*, *HLA-DPA1*, *HLA-DPB1*, *HLA-DQB1*, *HLA-DRA*, and *HLA-DRB1* were identified as the core hubs in the green module. The HLA allele polymorphisms influenced the susceptibility to RA.[36] High frequency expression of *HLA-DPB1*0401* and *0601* were identified as the risk factors, however low frequency expression of *DPB1*0101*, *0402*, and *0501* may be the protective factors for RA.[37] Moreover, *BLNK*, *BTK*, *CD3D*, *CD4*, *IL2RG*, *INPP5D*, *LCK*, *PTPRC*, *RAC2*, *SYK*, and *VAV1* were identified as the core hubs functionally relevant to the greenyellow module. Liubchenko et al[38] showed that decreased phosphorylation of BLNK was associated with the loss of anergic B cell tolerance in RA. During B cell development and

Table III. Potential therapeutic compound screening based on module analysis.

Compound	Module adjusted score*	Module number†	Rank‡
Niclosamide	2.01057	3	1
Anisomycin	2.00309	3	2
Lanatoside C	1.98056	4	3
Lycorine	1.95975	3	4
Helveticoside	1.87462	3	5
Cephaeline	1.81156	3	6
Phenoxybenzamine	1.76391	3	7
Lomustine	1.73451	3	8
Thapsigargin	1.71736	2	9
5,253,409	1.66515	2	10
Ikarugamycin	1.6206	2	11
Proscillaridin	1.60605	2	12
Lasalocid	1.58465	2	13
Oxyphenbutazone	1.476	2	14
Digitoxigenin	1.43979	3	15
Prestwick-1082	1.41483	2	16
Semustine	1.40952	2	17
STOCK1N-35696	1.40523	2	18
Nomegestrol	1.40221	2	19
Hexetidine	1.40123	2	20

*Compound enrichment scores adjusted by module-trait correlation coefficient.
†Targeted-module number of compounds.
‡Rank of compounds according to the module adjusted scores.

activation, *BTK* is involved in multiple signalling pathways downstream of the pre-B cell receptor (BCR) and Fc receptors (FcR), which is associated with RA.[39] Chang et al[40] found that *IL2RG* was differentially expressed in RA synovial tissues by RNA-sequencing. *INPP5D* was recognized as a negative regulator, which regulates interferon (IFN)-beta production downstream of toll-like receptor 3 (TLR3).[41] Romagnoli et al[42] showed a direct quantitative correlation between T cell hyporesponsiveness and modulation of LCK, a critical protein tyrosine kinase required for T cell activation. *PTPRC* rs10919563, a confirmed RA susceptibility locus, was the most replicated genetic biomarker of response to TNF inhibitors.[43] Dey et al[44] found that *RAC2* was up-regulated consistently in the RA synovium and revealed the interplay between *RAC2* and *STAT1* in the regulation of nitric oxide. The phosphorylation of SYK in peripheral blood B cells was greatly elevated in RA, accompanied by strong anti-citrullinated protein antibody (ACPA) positivity.[45] Guerreiro-Cacais et al[46] addressed the role of VAV1 in RA pathogenesis in experimental models and the patients of anti-cyclic citrullinated peptide (CCP)-negative RA.

In recent years, noncoding RNAs (ncRNAs) such as microRNAs (miRNAs) and lncRNAs are recognized as the emerging players in diverse biological processes and diseases including arthritis.[47,48] *FAM30A* showed its crucial role in the function of some immune cells, such as Th1, Th2, Th17, and natural killer cells (NK cells). Moreover, *CD3D*, *IL2RG*, *LCK*, and *HLA-DOB* presented

high functional connectivity with *FAM30A*, among which *CD3D*, *IL2RG*, and *LCK* are the core hub genes we identified. *NEAT1*-related hub genes were mainly involved in the MAPK pathway, among which *FGFR1* showed high functional connectivity with *NEAT1*. Zhang et al[49] identified the role of *NEAT1* in the TLR4-mediated inflammatory process, which affected the activation of the MAPK signalling pathway. Some studies[50–52] have indicated the roles of *FGFR1* in RA,[53] however the relationship between *FGFR1* and *NEAT1* has not been confirmed.

Given that some respond little to the RA pharmacological treatment and suffer from severe side effects,[1] we developed a novel algorithm based on modules to screen the promising drugs. In our study, we identified the drugs harbouring the opposite gene expression signature of RA-related modules and ranked them by the MAS, which ensures the high specificity and broad coverage for RA. Niclosamide, which had the highest MAS, was proven to be effective in the treatment of RA.[54] In an eight-week randomized controlled pilot study, Al-Gareeb et al[55] found that niclosamide was an adjuvant to etanercept for the Iraqi patients of active RA and greatly improved life quality, reduced the clinical assessment scoring indices, and decreased the serum level of IL-1β, E-selectin, vascular cell adhesion molecule 1 (VCAM1), and intercellular adhesion molecule 1 (ICAM1).[55] Niclosamide reduced the secretion of multiple cytokines from TNF-α-induced human RA fibroblast-like synoviocytes (FLS) and inhibited the migration and invasion of FLS by suppressing F-actin alterations. Moreover, niclosamide suppressed MAPK and nuclear factor kappa-light-chain-enhancer of activated B cells (NF-κB) pathway activity in FLS. The treatment effect was also confirmed in the collagen-induced arthritis mouse model.[56] Huang et al[57] confirmed that niclosamide induced mitochondrial apoptosis and inhibited proliferation of human RA fibroblast-like synoviocytes via the Akt signalling pathway.[57] Still, more clinical evidence and mechanism research is needed in future. Due to the variance of genetic background among ethnicities, the response to niclosamide should be considered among different ethnicities. In addition to oral administration, other types of drug delivery should be a valuable direction, such as intra-articular injection which may reduce the effective amount. Given that we constructed the mapping of niclosamide and modules, it is valuable to investigate the regulation between niclosamide and those hub genes in the modules, such as *BTK* and *LCK*, to reveal underlying molecular mechanisms.

In conclusion, we constructed a WGCNA to identify the significant RA-related modules and potential targets, the functional annotation of which revealed their indispensable roles in RA. To screen the promising drugs for RA, we developed a module-based and cumulatively scoring approach which ensured high specificity and broad coverage of RA-related modules. Our study provides not only the promising targets and drugs for RA

but also a novel methodological insight into the potential target and drug screening.

Supplementary material

ë Figure showing a dendrogram of the hierarchical clustering in the study, and table showing clinical features of the patients and healthy donors included.

References

1. **Burmester GR**, **Pope JE**. Novel treatment strategies in rheumatoid arthritis. *Lancet*. 2017;389(10086):2338–2348.

2. **Korani S**, **Korani M**, **Butler AE**, **Sahebkar A**. Genetics and rheumatoid arthritis susceptibility in Iran. *J Cell Physiol*. 2019;234(5):5578–5587.

3. **Simon TA**, **Thompson A**, **Gandhi KK**, **Hochberg MC**, **Suissa S**. Incidence of malignancy in adult patients with rheumatoid arthritis: a meta-analysis. *Arthritis Res Ther*. 2015;17:212.

4. **Hoovestol RA**, **Mikuls TR**. Environmental exposures and rheumatoid arthritis risk. *Curr Rheumatol Rep*. 2011;13(5):431–439.

5. **Eyre S**, **Bowes J**, **Diogo D**, **et al**. High-Density genetic mapping identifies new susceptibility loci for rheumatoid arthritis. *Nat Genet*. 2012;44(12):1336–1340.

6. **Sardar S**, **Andersson A**. Old and new therapeutics for rheumatoid arthritis: in vivo models and drug development. *Immunopharmacol Immunotoxicol*. 2016;38(1):2–13.

7. **Woetzel D**, **Huber R**, **Kupfer P**, **et al**. Identification of rheumatoid arthritis and osteoarthritis patients by transcriptome-based rule set generation. *Arthritis Res Ther*. 2014;16(2):R84.

8. **Chen YJ**, **Chang WA**, **Wu LY**, **et al**. Systematic analysis of differential expression profile in rheumatoid arthritis chondrocytes using next-generation sequencing and bioinformatics approaches. *Int J Med Sci*. 2018;15(11):1129–1142.

9. **Li WC**, **Bai DL**, **Xu Y**, **et al**. Identification of differentially expressed genes in synovial tissue of rheumatoid arthritis and osteoarthritis in patients. *J Cell Biochem*. 2019;120(3):4533-4544.

10. **Panga V**, **Raghunathan S**. A cytokine protein-protein interaction network for identifying key molecules in rheumatoid arthritis. *PLoS One*. 2018;13(6):e0199530.

11. **Langfelder P**, **Horvath S**. WGCNA: an R package for weighted correlation network analysis. *BMC Bioinformatics*. 2008;9:559.

12. **Ma C**, **Lv Q**, **Teng S**, **et al**. Identifying key genes in rheumatoid arthritis by weighted gene co-expression network analysis. *Int J Rheum Dis*. 2017;20(8):971–979.

13. **Lamb J**, **Crawford ED**, **Peck D**, **et al**. The connectivity map: using gene-expression signatures to connect small molecules, genes, and disease. *Science*. 2006;313(5795):1929–1935.

14. **Qu XA**, **Rajpal DK**. Applications of connectivity map in drug discovery and development. *Drug Discov Today*. 2012;17(23-24):1289–1298.

15. **Subramanian A**, **Narayan R**, **Corsello SM**, **et al**. A next generation connectivity map: L1000 platform and the first 1,000,000 profiles. *Cell*. 2017;171(6):1437–1452.

16. **Joerger M**, **Baty F**, **Früh M**, **et al**. Circulating microRNA profiling in patients with advanced non-squamous NSCLC receiving bevacizumab/erlotinib followed by platinum-based chemotherapy at progression (SAKK 19/05). *Lung Cancer*. 2014;85(2):306–313.

17. **Papiez A**, **Marczyk M**, **Polanska J**, **Polanski A**. BatchI: batch effect identification in high-throughput screening data using a dynamic programming algorithm. *Bioinformatics*. 2019;35(11):1885–1892.

18. **Yu G**, **Wang LG**, **Han Y**, **He QY**. clusterProfiler: an R package for comparing biological themes among gene clusters. *OMICS*. 2012;16(5):284–287.

19. **Fang S**, **Zhang L**, **Guo J**, **et al**. NONCODEV5: a comprehensive annotation database for long non-coding RNAs. *Nucleic Acids Res*. 2018;46(D1):D308–D314.

20. **Mathew AJ**, **Ravindran V**. Infections and arthritis. *Best Pract Res Clin Rheumatol*. 2014;28(6):935–959.

21. **Quaresma JAS**, **Yoshikawa GT**, **Koyama RVL**, **et al**. HTLV-1, immune response and autoimmunity. *Viruses*. 2015;8(1):5.

22. **Umekita K**, **Hidaka T**, **Miyauchi S**, **et al**. Treatment with anti–tumor necrosis factor biologic agents in human T lymphotropic virus type I–positive patients with rheumatoid arthritis. *Arthritis Care Res (Hoboken)*. 2014;66(5):788–792.

23. **Büchel F**, **Mittag F**, **Wrzodek C**, **et al**. Integrative pathway-based approach for genome-wide association studies: identification of new pathways for rheumatoid arthritis and type 1 diabetes. *PLoS One*. 2013;8(10):e78577.

24. **Us T**, **Cetin E**, **Kaşifoğlu N**, **Kaşifoğlu T**, **Akgün Y**. Investigation of Epstein-Barr virus and herpes simplex virus markers by serological and molecular methods in patients with rheumatoid arthritis and systemic lupus erythematosus. *Mikrobiyol Bul*. 2011;45(4):677–683. (Article in Turkish).

25. **Armangue T**, **Leypoldt F**, **Málaga I**, **et al**. Herpes simplex virus encephalitis is a trigger of brain autoimmunity. *Ann Neurol*. 2014;75(2):317–323.

26. **Greco A**, **Gallo A**, **Fusconi M**, **et al**. Bell's palsy and autoimmunity. *Autoimmun Rev*. 2012;12(2):323–328.

27. **Bedoya SK**, **Lam B**, **Lau K**, **Larkin J**. Th17 cells in immunity and autoimmunity. *Clin Dev Immunol*. 2013;2013:986789.:1–16.

28. **Atta AM**, **Carvalho EM**, **Jerônimo SMB**, **Sousa Atta MLB**. Serum markers of rheumatoid arthritis in visceral leishmaniasis: rheumatoid factor and anti-cyclic citrullinated peptide antibody. *J Autoimmun*. 2007;28(1):55–58.

29. **Corrotte M**, **Nyguyen APT**, **Harlay ML**, **et al**. Ral isoforms are implicated in Fc gamma R-mediated phagocytosis: activation of phospholipase D by RalA. *J Immunol*. 2010;185(5):2942–2950.

30. **Zhang M**, **Mu H**, **Lv H**, **et al**. Integrative analysis of genome-wide association studies and gene expression analysis identifies pathways associated with rheumatoid arthritis. *Oncotarget*. 2016;7(8):8580–8589.

31. **Luan M**, **Shang Z**, **Teng Y**, **et al**. The shared and specific mechanism of four autoimmune diseases. *Oncotarget*. 2017;8(65):108355–108374.

32. **Torsteinsdóttir I**, **Arvidson NG**, **Hällgren R**, **Håkansson L**. Monocyte activation in rheumatoid arthritis (rA): increased integrin, Fc gamma and complement receptor expression and the effect of glucocorticoids. *Clin Exp Immunol*. 1999;115(3):554–560.

33. **Brun JG**, **Madland TM**, **Vedeler CA**. Immunoglobulin G Fc-receptor (FcgammaR) IIA, IIIa, and IIIB polymorphisms related to disease severity in rheumatoid arthritis. *J Rheumatol*. 2002;29(6):1135–1140.

34. **Santegoets KCM**, **Wenink MH**, **van den Berg WB**, **Radstake TRDJ**. Fc gamma receptor IIb on GM-CSF macrophages controls immune complex mediated inhibition of inflammatory signals. *PLoS One*. 2014;9(10):e110966.

35. **Glossop JR**, **Emes RD**, **Nixon NB**, **et al**. Genome-wide DNA methylation profiling in rheumatoid arthritis identifies disease-associated methylation changes that are distinct to individual T- and B-lymphocyte populations. *Epigenetics*. 2014;9(9):1228–1237.

36. **Mariaselvam CM**, **Fortier C**, **Charron D**, **et al**. HLA class II alleles influence rheumatoid arthritis susceptibility and autoantibody status in South Indian Tamil population. *HLA*. 2016;88(5):253–258.

37. **Jiang L**, **Jiang D**, **Han Y**, **Shi X**, **Ren C**. Association of HLA-DPB1 polymorphisms with rheumatoid arthritis: A systemic review and meta-analysis. *Int J Surg*. 2018;52:98–104.

38. **Liubchenko GA**, **Appleberry HC**, **Striebich CC**, **et al**. Rheumatoid arthritis is associated with signaling alterations in naturally occurring autoreactive B-lymphocytes. *J Autoimmun*. 2013;40:111–121.

39. **Whang JA**, **Chang BY**. Bruton's tyrosine kinase inhibitors for the treatment of rheumatoid arthritis. *Drug Discov Today*. 2014;19(8):1200–1204.

40. **Chang X**, **Yue L**, **Liu W**, **et al**. CD38 and E2F transcription factor 2 have uniquely increased expression in rheumatoid arthritis synovial tissues. *Clin Exp Immunol*. 2014;176(2):222–231.

41. **Gabhann JN**, **Higgs R**, **Brennan K**, **et al**. Absence of SHIP-1 results in constitutive phosphorylation of tank-binding kinase 1 and enhanced TLR3-dependent IFN-beta production. *J Immunol*. 2010;184(5):2314–2320.

42. **Romagnoli P**, **Strahan D**, **Pelosi M**, **Cantagrel A**, **van Meerwijk JP**. A potential role for protein tyrosine kinase p56(lck) in rheumatoid arthritis synovial fluid T lymphocyte hyporesponsiveness. *Int Immunol*. 2001;13(3):305–312.

43. **Ferreiro-Iglesias A**, **Montes A**, **Perez-Pampin E**, **et al**. Replication of PTPRC as genetic biomarker of response to TNF inhibitors in patients with rheumatoid arthritis. *Pharmacogenomics J*. 2016;16(2):137–140.

44. **Dey P**, **Panga V**, **Raghunathan S**. A cytokine signalling network for the regulation of inducible nitric Oxide synthase expression in rheumatoid arthritis. *PLoS One*. 2016;11(9):e0161306.

45. **Iwata S**, **Nakayamada S**, **Fukuyo S**, **et al**. Activation of Syk in peripheral blood B cells in patients with rheumatoid arthritis: a potential target for abatacept therapy. *Arthritis Rheumatol*. 2015;67(1):63–73.

46. **Guerreiro-Cacais AO**, **Norin U**, **Gyllenberg A**, **et al**. VAV1 regulates experimental autoimmune arthritis and is associated with anti-CCP negative rheumatoid arthritis. *Genes Immun*. 2017;18(1):48–56.

47. **Yin CM**, **Suen WC**, **Lin S**, **et al**. Dysregulation of both miR-140-3p and miR-140-5p in synovial fluid correlate with osteoarthritis severity. *Bone Joint Res*. 2017;6(11):612–618.

48. **Li H**, **Yang HH**, **Sun ZG**, **Tang HB**, **Min JK**. Whole-transcriptome sequencing of knee joint cartilage from osteoarthritis patients. *Bone Joint Res*. 2019;8(7):290–303.

49. **Zhang F**, **Wu L**, **Qian J**, **et al**. Identification of the long noncoding RNA NEAT1 as a novel inflammatory regulator acting through MAPK pathway in human lupus. *J Autoimmun*. 2016;75:96–104.

50. **Byrd V**, **Zhao XM**, **McKeehan WL**, **Miller GG**, **Thomas JW**. Expression and functional expansion of fibroblast growth factor receptor T cells in rheumatoid synovium and peripheral blood of patients with rheumatoid arthritis. *Arthritis Rheum*. 1996;39(6):914–922.

51. **Zhang L**, **Li W**, **Song L**, **Chen L**. A towards-multidimensional screening approach to predict candidate genes of rheumatoid arthritis based on SNP, structural and functional annotations. *BMC Med Genomics*. 2010;3(1):38.

52. **Qin S**, **Sun D**, **Li H**, **et al**. The Effect of SHH-Gli Signaling Pathway on the Synovial Fibroblast Proliferation in Rheumatoid Arthritis. *Inflammation*. 2016;39(2):503–512.

53. **Tan Q**, **Chen B**, **Wang Q**, **et al**. A novel FGFR1-binding peptide attenuates the degeneration of articular cartilage in adult mice. *Osteoarthritis Cartilage*. 2018;26(12):1733–1743.

54. **Chen W**, **Mook RA**, **Premont RT**, **Wang J**. Niclosamide: Beyond an antihelminthic drug. *Cell Signal*. 2018;41:89–96.

55. **Al-Gareeb AIA**, **Gorial FI**, **Mahmood AS**. Niclosamide as an adjuvant to etanercept in treatment patients with active rheumatoid arthritis: an 8-week randomized controlled pilot study. *Clin Rheumatol*. 2018;37(10):2633–2641.

56. **Liang L**, **Huang M**, **Xiao Y**, **et al**. Inhibitory effects of niclosamide on inflammation and migration of fibroblast-like synoviocytes from patients with rheumatoid arthritis. *Inflamm Res*. 2015;64(3-4):225–233.

57. **Huang M**, **Zeng S**, **Qiu Q**, **et al**. Niclosamide induces apoptosis in human rheumatoid arthritis fibroblast-like synoviocytes. *Int Immunopharmacol*. 2016;31:45–49.

Author information:
- X. Li, MD, Associate Chief Physician
- Y. Yang, MD, Associate Chief Physician
- W. Dai, MD, Postgraduate
- Y. Du, MD, Attending Physician

  Department of Bone and Joint Surgery, The Third Affiliated Hospital of Guangxi Medical University, Nanning, China.
- G. Sun, MD, Associate Chief Physician, Department of Nutriology, The Third Affiliated Hospital of Guangxi Medical University, Nanning, China.
- X. Jie, MD, Chief Physician, Department of Hematology, The Third Affiliated Hospital of Guangxi Medical University, Nanning, China.
- R. Huang, MD, Undergraduate, Second Clinical College, Tongji Hospital, Tongji Medical College, Huazhong University of Science and Technology, Wuhan, China.
- J. Zhang, MD, Resident Physician, Department of Orthopedics, Tongji Hospital, Tongji Medical College, Huazhong University of Science and Technology, Wuhan, China; Cancer Center, Union Hospital, Tongji Medical College, Huazhong University of Science and Technology, Wuhan, China.

Author contributions:
- X. Li: Wrote and revised the manuscript.
- Y. Yang: Wrote the manuscript.
- G. Sun: Analyzed the data.
- W. Dai: Analyzed the data.
- X. Jie: Analyzed the data.
- Y. Du: Analyzed the data.
- R. Huang: Analyzed the data.
- J. Zhang: Designed the study, Analyzed the data, Gave the final approval of the manuscript.

  X. Li and Y. Yang contributed equally to this work.